Desalination and Water Treatment
www.deswater.com
doi: 10.1080/19443994.2014.934727

56 (2015) 256–265
September

Taylor & Francis
Taylor & Francis Group

Effective removal of cadmium ions from aqueous solution using chitosan-stabilized nano zero-valent iron

Hongfei Lu, Xueliang Qiao*, Wei Wang, Fatang Tan, Fazhe Sun, Zunqi Xiao, Jianguo Chen

State Key Laboratory of Material Processing and Die and Mould Technology, Huazhong University of Science and Technology, Wuhan 430074, P.R. China, Tel./Fax: +86 27 87541540; emails: 315079006@qq.com (H. Lu), hflu2011@163.com (X. Qiao), weiwang@hust.edu.cn (W. Wang), fatangtan@hust.edu.cn (F. Tan), 279629842@qq.com (F. Sun), 364884637@qq.com (Z. Xiao), jgchen5711@163.com (J. Chen)

Received 21 November 2013; Accepted 2 June 2014

ABSTRACT

In this study, a series of chitosan-stabilized nano zero-valent iron (CNZVI) composites with different amounts of chitosan were prepared and characterized by Fourier transform infrared spectra, X-ray diffraction, and transmission electron microscopy. The adsorption capacity of these composites was evaluated by the removal experiment of cadmium ion (Cd^{2+}) from aqueous solution. These results showed that the as-prepared $CNZVI_8$ composite with loose aggregate structure has the maximum adsorption capacity for Cd^{2+}. Furthermore, batch adsorption experiments of Cd^{2+} on $CNZVI_8$ composite were performed under various conditions, such as contact time, adsorbent dosage, initial Cd^{2+} concentration, and the initial pH of solution. The data revealed that the maximum adsorption capacity of $CNZVI_8$ is 124.74 mg/g. The removal efficiency of Cd^{2+} increased with the increase in solution pH value, and reaches 99.9% at pH 6. In addition, the adsorption isotherm and the adsorption kinetics of Cd^{2+} on $CNZVI_8$ were also investigated, suggesting that the isothermal data were well fitted to the Langmuir model and the kinetic data were well suitable to the pseudo-second-order kinetic model.

Keywords: Nano zero-valent iron; Chitosan; Adsorption; Cadmium ion

1. Introduction

Heavy metal ions pollutants in the aquatic environment have been concerned intensively due to their acute toxicity and their accumulation effect in living beings. Cadmium ion (Cd^{2+}) is one of the most toxic pollutants in aquatic systems [1], which could pose a serious threat to human health, such as diarrhea, nausea, muscle cramps, damage of bone marrow, and formation of kidney stones, due to its nonbiological degradation property and accumulation in plants and animals through food chain relationships [2]. Several removal technologies of Cd^{2+} have been reported, such as membrane filtration [3,4], reverse osmosis [5], precipitation [6], electrochemical deposition, and ion exchange [7]. Nevertheless, the application of these technologies is limited because of its low efficiency, high cost, and complicated operation.

Adsorption is a promising and widely applied technology in the removal of heavy metals, since it is

*Corresponding author.

economical and effective [8–10]. Recently, nano zero-valent iron (NZVI) has been considered to be an excellent adsorbent for removing heavy metal ions due to its high adsorption capacity [11], low cost [12], controlling over the secondary pollutants [13], and nontoxic final products. However, the bare NZVI particles can easily be oxidized and aggregated because of its high activity and intrinsic magnetism [14]. Thus, many researchers have prepared NZVI using polymers or surfactants as stabilizers to solve these problems [14–17]. It is well known that chitosan is an excellent stabilizer due to its hydrophilicity, biodegradability, and nontoxicity [18]. There have been some reports about using chitosan-stabilized NZVI (CNZVI) to remove heavy metal ions, such as hexavalent chromium [19,20], inorganic arsenic [21], and lead and copper ions [22]. To the best of our knowledge, there were little reports about using CNZVI for the removal of Cd^{2+}, and even there were no literatures studying the amount of chitosan affecting on the adsorption capacity of NZVI.

Herein, we prepared a series of CNZVI composites by varying the amounts of chitosan. The effect of the amount of chitosan on the morphologies and structures of CNZVI composites was investigated by Fourier transform infrared spectra (FTIR), X-ray diffraction (XRD), and transmission electron microscopy (TEM). The adsorption capacity of these CNZVI composites was evaluated through the removal of Cd^{2+} from aqueous solution. Furthermore, the effects of contact time, initial solution pH, initial Cd^{2+} concentrations, and adsorbent dosage on the removal of Cd^{2+} were studied in detailed. Langmuir and Freundlich models were applied to discuss the adsorption isotherm of Cd^{2+} on CNZVI in order to explain the adsorption mechanism. Pseudo-first-order and pseudo-second-order models were used to investigate the adsorption kinetics of the removal of Cd^{2+} on CNZVI.

2. Materials and methods

2.1. Materials

All the required chemicals in the study were of analytical grade and were used without further purification. Ferrous sulfate heptahydrate ($FeSO_4 \cdot 7H_2O$) 99%, sodium borohydride ($NaBH_4$) 96%, cadmium chloride ($CdCl_2 \cdot 2.5H_2O$) 99%, and chitosan flakes (80–95% deacetylation) were acquired from Sinopharm Chemical Reagent Co., Ltd. The stock solution containing 100 mg/L of Cd^{2+} was prepared by dissolving an appropriate amount of $CdCl_2 \cdot 2.5\ H_2O$ with distilled water and the solution pH was adjusted by adding 1.0 mol/L of hydrochloric acid (HCl) and 1.0 mol/L of sodium hydroxide (NaOH).

2.2. Preparation of CNZVI

Before the preparation of CNZVI, distilled water was purged with high-purity argon for 1 h so that the dissolved oxygen would fall to a level below 0.5 mg/L. CNZVI was prepared in a 250 mL flask reactor with three open necks. The detailed procedure was as follows: initially, 11.2 mg of chitosan was added into 50 mL of distilled water using acetic acid (2%) to facilitate dissolving. Then, 2.78 g (10 mmol) of $FeSO_4 \cdot 7H_2O$ was added to the solution, the mixture was stirred vigorously (250 rpm) for 30 min. Finally, to this mixture solution, 50 mL of freshly prepared aqueous solution containing 1.14 g (30 mmol) of $NaBH_4$ was added. The reduction reaction is expressed in Eq. (1):

$$Fe^{2+} + 2BH_4^- + 6H_2O \rightarrow Fe^0 + 2B(OH)_3 + 7H_2 \uparrow \quad (1)$$

After the $NaBH_4$ solution was added, the mixture was stirred for another 30 min, the nano-iron slurry was collected by magnetism. The collected slurry was washed three times by deoxygenated water, absolute ethanol, and acetone, respectively. The whole process was carried out in an argon atmosphere. The products were dried under vacuum conditions. Similarly, the other CNZVI samples were prepared by varying the amount of chitosan from 22.4 to 67.2 mg while keeping the rest constant.

2.3. Characterization of CNZVI

The particle size, morphology, and crystallinity of the CNZVI samples were characterized using TEM (JEOL JEM-100CXⅡ with an accelerating voltage of 100 kV) and XRD (Philips X'Pert PRO with the Cu-Kα radiation and the accelerating voltage of 40 kV, emission current of 40 mA). The chitosan on the nanoparticle surface was analyzed using FTIR (Bruker VERTEX 70).

2.4. Batch adsorption experiments

Argon gas was blown into the flasks to maintain an anoxic condition during the reaction and the flasks were shaken at 250 rpm for 24 h using a thermostatic shaker at room temperature. The pH value of the Cd^{2+} stock solution was about 5.6. To investigate the adsorption capacity of as-prepared CNZVI samples towards Cd^{2+}, 25 mL of Cd^{2+} stock solution was

added to a series of Erlenmeyer flasks and then 30 mg of different CNZVI samples was added to the solution, respectively. To investigate the effect of the contact time, 250 mL of Cd^{2+} stock solution was filled into a 500 mL Erlenmeyer flask and 200 mg of CNZVI was added to the flask. Samples were taken out at various time intervals. To investigate the effect of the adsorbent dosage, batch adsorption experiments were conducted with 25 mL of Cd^{2+} stock solution; the amount of adsorbent was added varying from to 2.5 to 30 mg. To investigate the effect of pH, taking 25 mL of Cd^{2+} stock solution into a series of Erlenmeyer flasks, the pH value of the solutions were adjusted from 2 to 7 by dropping 1.0 mol/L HCl or 1.0 mol/L NaOH solution and then 30 mg of adsorbent were added, respectively. To investigate the effect of initial metal ions concentration, 100 mg of CNZVI was added to 25 mL of Cd^{2+} solution with varying the concentration from 50 to 1,000 mg/L.

After each test, samples were taken out and filtered through a membrane of 0.25 μm pore size. The concentration of Cd^{2+} in the filtrate was measured with voltammetric analysis system (VAS, PDV6000 *plus*, Cogent Environmental Ltd, UK).

The removal efficiency of Cd^{2+} and the adsorbed amount of CNZVI were determined by the following Eqs. (2) and (3), respectively:

$$\text{Removal}\,(\%) = \frac{(C_0 - C_t)}{C_0} \times 100 \tag{2}$$

$$q_t = \frac{(C_0 - C_t)V}{m} \tag{3}$$

where C_0 and C_t (mg/L) are the Cd^{2+} concentrations in solution at the initial time and at any time t, respectively; m (g) is the weight of CNZVI; and V (mL) is the volume of the solution. In these equations, C_e is the equilibrium concentration and q_e is the adsorption amount of Cd^{2+} at equilibrium time.

3. Results and discussion

3.1. Characterization of CNZVI samples

Fig. 1 presents the FTIR spectra of the chitosan and CNZVI samples. The main bands in the IR spectra of chitosan can be seen as follows: a broad band at around 3,442 cm^{-1} (O–H and N–H stretching vibrations); a weak band at 2,896 cm^{-1} (C–H stretching vibrations); a band at 1,652 cm^{-1} (C–N stretching vibrations); and middle strong bands at around 1,390 cm^{-1} (–C–O stretching of primary alcoholic group), 1,155 cm^{-1} (bridged-oxygen stretching vibrations), and 1,087 cm^{-1}

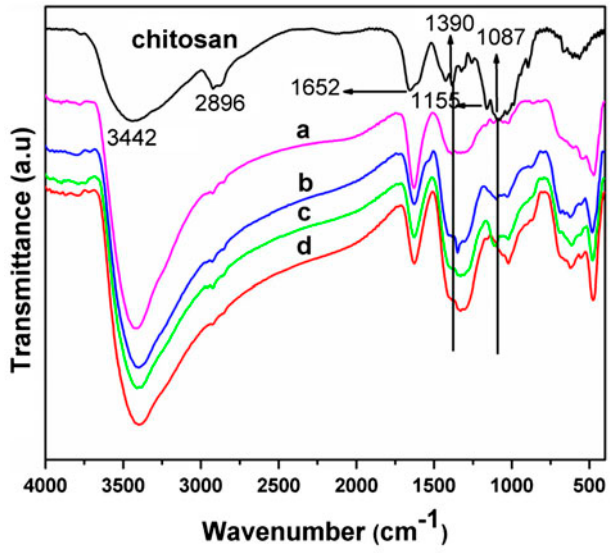

Fig. 1. FTIR spectra of chitosan and the CNZVI samples with different of m_c/m_i: (a) $m_c/m_i = 0$; (b) $m_c/m_i = 0.04$; (c) $m_c/m_i = 0.08$; and (d) $m_c/m_i = 0.12$.

(N–H stretching vibrations) [23]. And, the FTIR spectra of CNZVI samples (Fig. 1 (b)–(d)) show that the characteristic bands of chitosan at 1,390 and 1,087 cm^{-1} shift to the low-wavenumber side. Moreover, it is noticed that the intensity of peaks at 1,390 and 1,087 cm^{-1} in the IR spectra of samples *b*, *c*, and *d* gradually increases with the increase in the mass ratio of chitosan to iron ions (m_c/m_i). The results clearly show that chitosan is adsorbed to the surface of the NZVI nanoparticles [24,25].

Fig. 2 shows the XRD patterns of CNZVI composites. The nano iron particles in these composites are in zero-valent state, as confirmed by a broad diffraction peak at $2\theta = 44.7^\circ$ [26]. Compared with the diffraction peak of sample *a*, the peaks of sample *b*, *c*, and *d* are significantly broadened and their intensities decrease with the increase in m_c/m_i, which also confirms that nano iron particles are stabilized by chitosan, and the amount of chitosan on the surface of nano iron particles is increasing [27]. In addition, the diffraction peak is broadened, suggesting that the iron particles are nanometer in size [28].

The TEM images of CNZVI composites are shown in Fig. 3. As presented in Fig. 3(a), the NZVI particles without stabilization by chitosan formed bulk and chain-like aggregates due to the strong van der Waals attraction with the high Hamaker constant of the magnetite shell as well as the magnetic attractions between the particles [29]. While Fig. 3(b)–(d) shows that the aggregate extent of NZVI particles is decreasing and the chain-like structure is much clear with the

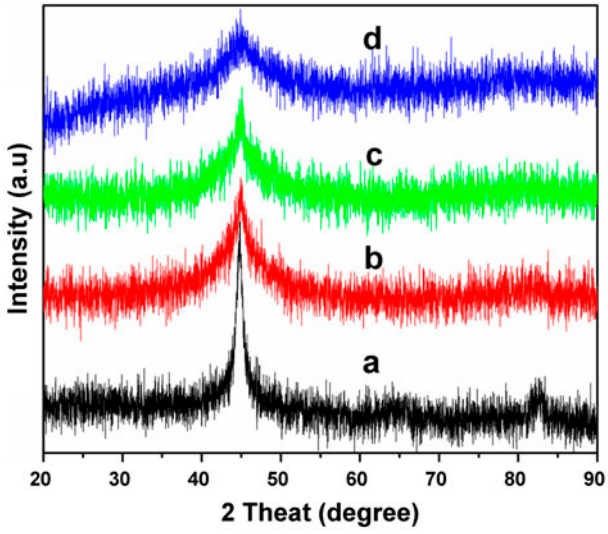

Fig. 2. XRD patterns of the CNZVI samples with different of m_c/m_i: (a) $m_c/m_i = 0$; (b) $m_c/m_i = 0.04$; (c) $m_c/m_i = 0.08$; and (d) $m_c/m_i = 0.12$.

increasing in m_c/m_i. It is worth noting that Fig. 3(c) shows a loose chain-like aggregate, which indicates that $m_c/m_i = 0.08$ is appropriate. Whereas, Fig. 3(d) presents a bold and long chain-like structure, revealing that many NZVI particles are encapsulated by chitosan. It is because the amount of chitosan is excessive in this CNZVI composite. All of these results also can be confirmed by the spectra of FTIR and the patterns of XRD.

3.2. *Adsorption capacity of the prepared CNZVI samples towards Cd^{2+}*

As described above, the m_c/m_i has an important effect on the morphologies and structures of CNZVI composites. Therefore, batch removal experiments of Cd^{2+} were conducted to investigate the adsorption capacity of CNZVI samples with different m_c/m_i ratios. The results are shown in Fig. 4. It is clearly seen that the removal efficiency of CNZVI samples towards Cd^{2+} increases with the increasing in m_c/m_i, whereas, it is decreasing when the value of m_c/m_i is more than 0.08. The results can be illustrated that NZVI particles without stabilized by chitosan tend to aggregate, which resulted in decreasing of the adsorption capacity of NZVI. Chitosan as a stabilizer was adsorbed on the surface of NZVI particles (Fig. 3), which could suppress the aggregation and oxidation of NZVI particles, resulting in increasing in the surface area and adsorption activity of CNZVI composites. However, in the presence of excessive chitosan, a thicker coating would be formed on the surface of NZVI, which would decrease the adsorption capacity of CNZVI towards Cd^{2+}.

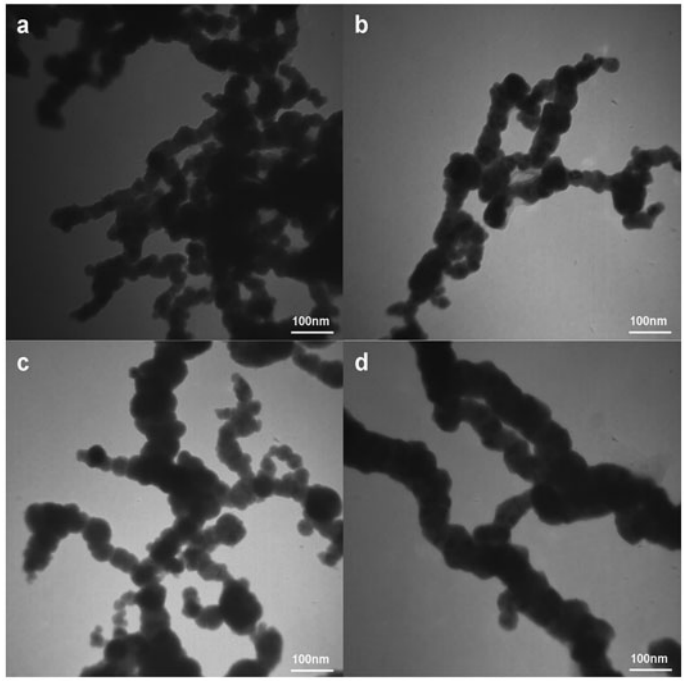

Fig. 3. TEM images of the CNZVI samples with different of m_c/m_i: (a) $m_c/m_i = 0$; (b) $m_c/m_i = 0.04$; (c) $m_c/m_i = 0.08$; and (d) $m_c/m_i = 0.12$.

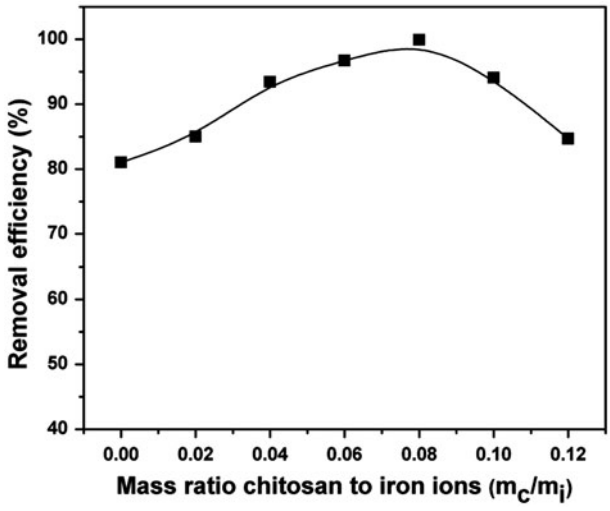

Fig. 4. Cd^{2+} adsorption on CNZVI samples with different of m_c/m_i (Experimental conditions: initial Cd^{2+} concentration = 100 mg/L; solution volume = 25 mL; pH 5.6; CNZVI = 30 mg).

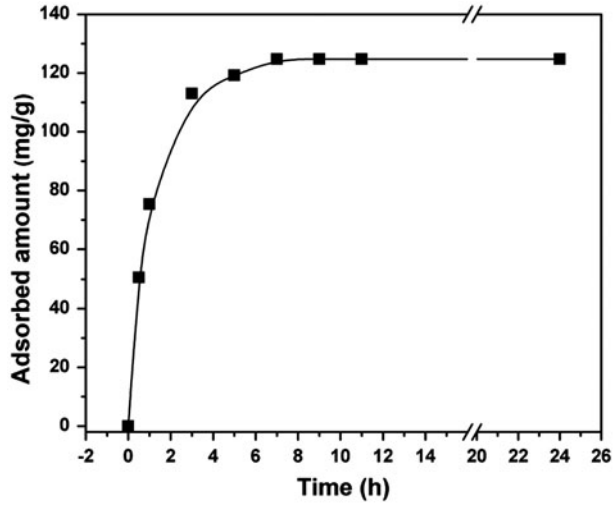

Fig. 5. Effect of contact time on Cd^{2+} adsorption (Experimental conditions: initial Cd^{2+} concentration = 100 mg/L; solution volume = 250 mL; pH 5.6; $CNZVI_8$ = 200 mg).

As shown in Fig. 4, the adsorption capacity of CNZVI sample is maximum when the value of m_c/m_i is 0.08. Therefore, this CNZVI sample is named as $CNZVI_8$ and used as an adsorbent to investigate other impact factors for the removal of Cd^{2+}.

3.3. Batch Cd^{2+} adsorption experiments

3.3.1. Effect of contact time

The time-course profile for the adsorption of Cd^{2+} on $CNZVI_8$ is given in Fig. 5. It can be seen that Cd^{2+} is adsorbed rapidly during the first 3 h, the adsorption equilibrium is attained within 7 h and the adsorbed amount do not change with further increase in contact time. It can be explained that there are lots of active sites of adsorbent and the concentration of Cd^{2+} is high at the initial stage; the adsorption active sites can rapidly interact with Cd^{2+}. After 3 h, the adsorbed amount is slowly increased until it reaches a constant value due to the slow diffusion of metal ions to the adsorbent and the reducing of active sites [30]. Additionally, adsorption equilibrium is a dynamic-balanced process which is affected by desorption [31]. Therefore, in order that it is sufficient to ensure apparent equilibrium, 24 h is selected as contact time for all of other experiments.

3.3.2. Effect of adsorbent dosage

The amount of adsorbent is chosen as a variable to study the adsorption of Cd^{2+}. Fig. 6 shows the removal efficiency and adsorbed amount for the adsorption of Cd^{2+} on $CNZVI_8$ with respect to the mass ratio of adsorbent to cadmium ions. The removal efficiency of Cd^{2+} is very low when the mass ratio of adsorbent to cadmium ions is 1. It is because adsorption active sites are few at low adsorbent amount, and the reaction between the adsorbent and the oxidizing species in solution also makes active sites decreasing. However, the removal efficiency of Cd^{2+} increases with the increase in the mass ratio of adsorbent to cadmium ions. It is attributed to the adsorption active sites increase with the increase in the amount of adsorbent. Nevertheless, the adsorbed amount of per unit mass of adsorbent decreases as the mass ratio of

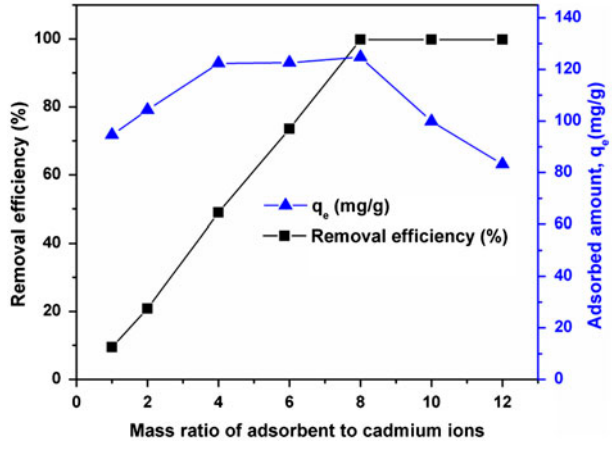

Fig. 6. Effect of adsorbent dosage on Cd^{2+} adsorption (Experimental conditions: initial Cd^{2+} concentration = 100 mg/L; solution volume = 25 mL; pH 5.6).

adsorbent to cadmium ions increases from 10 to 12. At a higher adsorbent dosage, the adsorption activity sites would be excessive for the demand of Cd^{2+} adsorption reaction, which leads to the unsaturation of the adsorption sites, resulting in relatively less adsorption amount [32].

3.3.3. Effect of initial solution pH

Fig. 7 shows the removal efficiency of Cd^{2+} with respect to the pH of initial solution. If the concentration of Cd^{2+} in solution is 100 mg/L, it would generate insoluble species at pH > 8 according to the solubility product of $Cd(OH)_2$. Therefore, the pH value in the range of 2–7 is selected for investigating the removal of Cd^{2+}. As shown in Fig. 7, the removal efficiency of Cd^{2+} increases with the increasing in pH value and the Cd^{2+} is almost completely removed at pH > 5. It can be interpreted that the surface charge of adsorbent becomes relatively more negative with the increase in the pH value of the solution [33], which is favorable for Cd^{2+} adsorption on adsorbent.

The changes of solution pH were also studied. From Fig. 7 (blue curve), it can be seen that the final pH value of the solution is increased, it is because NZVI reacts with H^+ and H_2O to give Fe^{2+} and OH^- according to Eqs. (4) and (5) [34].

$$2Fe^0 + 4H^+ + O_2 \rightarrow 2Fe^{2+} + 2H_2O \quad (4)$$

$$2Fe^0 + O_2 + 2H_2O \rightarrow 2Fe^{2+} + 4OH^- \quad (5)$$

3.3.4. Effect of initial metal ion concentration

The effect of initial metal ion concentration on the removal of Cd^{2+} is shown in Fig. 8. With the increasing in initial Cd^{2+} concentration, the equilibrium adsorption amount of $CNZVI_8$ increases from 12.5 to 124.74 mg/g, whereas the removal efficiency decreases from 99.9 to 49.8%. At low initial concentration, the Cd^{2+} can be almost completely removed because there are sufficient adsorption sites on $CNZVI_8$ for the adsorption of Cd^{2+}. However, at higher Cd^{2+} concentration, the ratio of the number of Cd^{2+} to the number of available adsorption active sites is large and a progressively higher number of Cd^{2+} are taken up with the gradual filling up of the appropriate active sites [35]. Therefore, the adsorbed amount of $CNZVI_8$ is increasing, although the removal efficiency comes down.

3.4. Adsorption isotherm of Cd^{2+} on $CNZVI_8$

In order to predict the adsorption behavior of metal ions on adsorbent, Langmuir and Freundlich adsorption isotherm models are commonly used to fit the data of adsorption isotherm [36]. The linear forms of these two models are presented in Eqs. (6) and (7), respectively:

$$\frac{C_e}{q_e} = \frac{1}{K_L q_m} + \frac{C_e}{q_m} \quad (6)$$

$$\ln q_e = \ln K_F + \frac{1}{n} \ln C_e \quad (7)$$

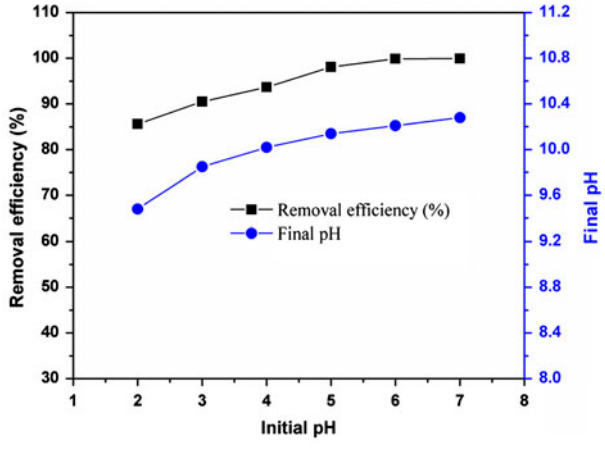

Fig. 7. Effect of initial solution pH on Cd^{2+} adsorption (Experimental conditions: initial Cd^{2+} concentration = 100 mg/L; solution volume = 25 mL; $CNZVI_8$ = 20 mg).

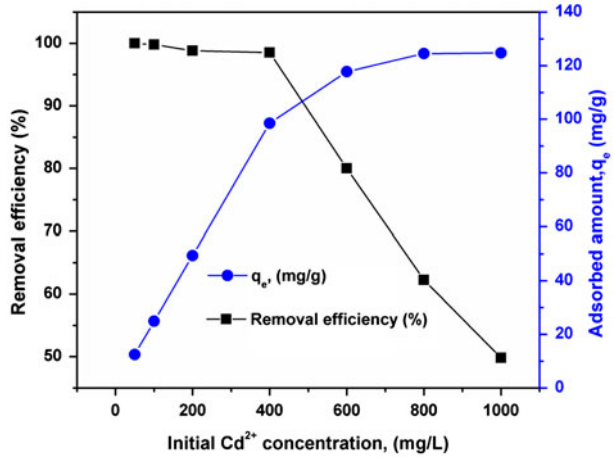

Fig. 8. Effect of initial metal ion concentration on Cd^{2+} adsorption (Experimental conditions: solution volume = 25 mL; pH 5.6; $CNZVI_8$ = 100 mg).

where q_e (mg/g) is the adsorbed amount of the adsorbent at equilibrium, C_e (mg/L) is the equilibrium concentration of Cd^{2+} in solution, q_m (mg/g) is the maximum adsorption capacity of the adsorbent, K_L (L/mg) is the Langmuir constant, and K_F ($mg^{1-1/n}L^{1/n}g^{-1}$) and n are Freundlich constants that were related to the adsorption capacity and the adsorption intensity, respectively.

Equilibrium adsorption isotherm studies were conducted with aqueous solutions of Cd^{2+}, varying the concentration from 50 to 1,000 mg/L and the adsorption equilibrium plot of Cd^{2+} on $CNZVI_8$ is shown in Fig. 9(a). The linear plots of Langmuir and Freundlich adsorption isotherms obtained at room temperature are presented in Fig. 9(b) and (c), respectively, and the adsorption parameters are listed in Table 1. The correlation coefficients (R^2) for Langmuir model and Frenudlich model are 0.9998 and 0.9349, respectively. Comparing the correlation coefficients, indicated that Langmuir model should describe the adsorption behavior of Cd^{2+} on $CNZVI_8$ better. Meanwhile, the adsorption capacity (q_m) calculated from Langmuir model is 126.58 mg/g, which is much closer to the experimental value (q_e). Thus, the adsorption of Cd^{2+} on $CNZVI_8$ is well fitted to the Langmuir isotherm model. Moreover, the value of n is 4.76, hence, the Freundlich constant $1/n$ is smaller than 1, it also indicates that this adsorption isotherm belongs to a normal Langmuir isotherm [37].

3.5. Adsorption kinetics of Cd^{2+} on $CNZVI_8$

Pseudo-first-order and pseudo-second-order kinetic models are usually used to investigate the adsorption kinetics of Cd^{2+} [38]. The linear forms of the models are presented in Eqs. (8) and (9), respectively:

$$\ln(q_e - q_t) = \ln q_e - k_1 t \tag{8}$$

$$\frac{t}{q_t} = \frac{1}{k_2 q_e^2} + \frac{1}{q_e} t \tag{9}$$

where q_e (mg/g) and q_t (mg/g) are the adsorbed amounts of the adsorbent at equilibrium and at any time t, t (h) is the contact time, and k_1 (h^{-1}) and k_2 ($mg\,g^{-1}\,h^{-1}$) are pseudo-first-order and pseudo-second-order rate constants, respectively.

According to the plot of adsorbed amount with respect to time (Fig. 5), the linear plots of ln ($q_e - q_t$) vs. t, and t/q_t vs. t are presented in Fig. 10(a) and (b), respectively. The parameters of the two kinetic models are summarized in Table 2. As can be observed, the

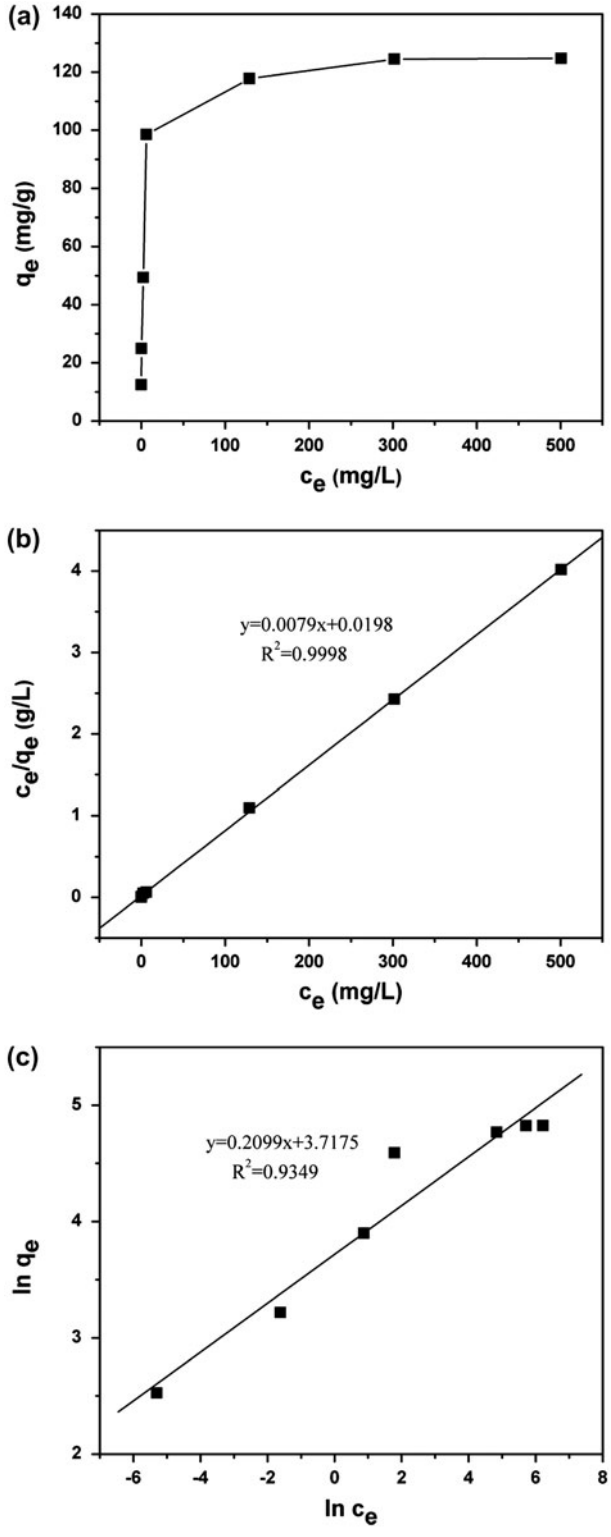

Fig. 9. Adsorption isotherms of Cd^{2+} on $CNZVI_8$: (a) equilibrium adsorption isotherms of Cd^{2+} on $CNZVI_8$; (b) Langmuir isotherm model plot; and (c) Freundlich isotherm model plot.

Table 1
Parameters of Langmuir and Freundlich adsorption isotherm models for Cd^{2+} on $CNZVI_8$

	Langmuir model			Freundlich model		
Temperature (K)	q_m (mg g^{-1})	K_L (L mg^{-1})	R^2	K_F (mg$^{1-1/n}$ L$^{1/n}$ g^{-1})	n	R^2
298	126.58	0.39	0.9998	41.16	4.76	0.9349

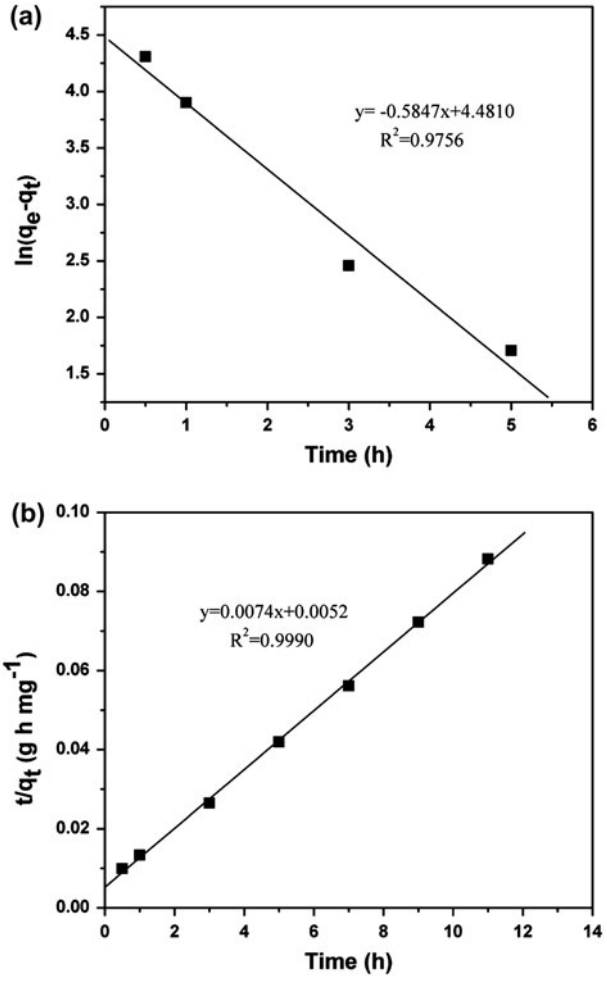

Fig. 10. Kinetics of Cd^{2+} adsorption on $CNZVI_8$: (a) pseudo-first-order model plot and (b) pseudo-second-order model plot.

theoretical adsorption amount ($q_{e,cal}$) of the pseudo-second-order kinetic model is much closer to the experimental value ($q_{e,exp}$) than that of the pseudo-first-order kinetic model. In addition, the correlation coefficient (R^2) of pseudo-second-order is better than that of pseudo-first-order kinetic model. Therefore, the pseudo-second-order model represented better the adsorption kinetics of Cd^{2+} on $CNZVI_8$ in contrast to the pseudo-first-order kinetic model. Similar trends have been reported for the adsorption of Cd^{2+} by other adsorbents [39,40].

3.6. Adsorption mechanism

The literature shows that the standard oxidation–reduction potential of Cd^{2+} ($E^0 = -0.40$) is very close to that of zero-valent iron ($E^0 = -0.41$), and the E^0 of Cd^{2+} is more positive than the Fermi energy (E_F) of zero-valent iron [41]. The reduction of Cd^{2+} is thermodynamically unfavorable. Therefore, there is no reduction of Cd^{2+} on the surface of CNZVI composite and the removal mechanism is purely sorption. Furthermore, according to the analysis of adsorption isotherm, the adsorption of Cd^{2+} on $CNZVI_8$ is fitted well with Langmuir model. While Langmuir model assumes that the surface of the adsorbent is homogenous and all adsorption active sites have identical energy, each adsorbate molecule has been located on a single site [42]. Hence, the adsorption of Cd^{2+} is monolayer adsorption on the surface of $CNZVI_8$ adsorbent. Additionally, the adsorption kinetics data justify that the adsorption of Cd^{2+} on $CNZVI_8$ followed the pseudo-second-order model, which implies that Cd^{2+} adsorption on $CNZVI_8$ may take place through a chemical process.

Table 2
Parameters of pseudo-first-order and pseudo-second-order kinetic models for Cd^{2+} on $CNZVI_8$

		Pseudo-first-order			Pseudo-second-order		
Temperature (K)	$q_{e,exp}$ (mg g^{-1})	k_1 (h^{-1})	$q_{e,cal}$ (mg g^{-1})	R^2	k_2 (g mg^{-1} h^{-1})	$q_{e,cal}$ (mg g^{-1})	R^2
298	124.74	0.5847	88.32	0.9756	0.0105	135.14	0.9990

4. Conclusions

In the present work, the effect of the mass ratio of chitosan to iron ions (m_c/m_i) on CNZVI characteristics and the adsorption capacity was evaluated. The results showed that the CNZVI composite formed loose aggregation and its adsorption capacity to Cd^{2+} is the maximum when the mass ratio of chitosan to iron ions is 0.08. Thus, this kind of CNZVI sample was used as an adsorbent to systematically investigate the removal of Cd^{2+} from aqueous solution. It was found that the maximum adsorption capacity of this kind of CNZVI composite to Cd^{2+} is 124.74 mg/g, and the removal efficiency of Cd^{2+} is influenced by the pH of solution, contact time, adsorbent dosage, and initial concentration of Cd^{2+} solution. Furthermore, Langmuir model was well fitted with the adsorption isotherm data, which indicated the formation of monolayer coverage of Cd^{2+} at the surface of $CNZVI_8$. The kinetic data justified that the adsorption of Cd^{2+} on $CNZVI_8$ followed the pseudo-second-order kinetic model. Consequently, fundamentally the outlook is promising that the $CNZVI_8$ composite is a potential candidate for the removal of Cd^{2+} from aqueous solution.

Acknowledgment

We gratefully acknowledge support of this research by the Analysis and Test center of HUST (Huazhong University of Science and Technology).

References

[1] H. Wang, Y. Jia, S. Wang, H. Zhu, X. Wu, Bioavailability of cadmium adsorbed on various oxides minerals to wetland plant species *Phragmites australis*, J. Hazard. Mater. 167 (2009) 641–646.
[2] A. Penkova, J. Martínez Blanes, S. Cruz, M. Centeno, K. Hadjiivanov, J. Odriozola, Gold nanoparticles on silica monospheres modified by amino groups, Microporous Mesoporous Mater. 117 (2009) 530–534.
[3] B. Al-Rashdi, D. Johnson, N. Hilal, Removal of heavy metal ions by nanofiltration, Desalination 315 (2013) 2–17.
[4] Y. Ahn, M.-G. Ha, Y.-J. Choi, Adsorptive behavior of acrylic acid-grafted bacterial cellulose to remove cadmium for a membrane-adsorbent hybrid process, Desalin. Water Treat. 51 (2013) 5074–5079.
[5] M.D. Afonso, J.O. Jaber, M.S. Mohsen, Brackish groundwater treatment by reverse osmosis in Jordan, Desalination 164 (2004) 157–171.
[6] J.O. Esalah, M.E. Weber, J.H. Vera, Removal of lead, cadmium and zinc from aqueous solutions by precipitation with sodium Di-(*n*-octyl) phosphinate, Can. J. Chem. Eng. 78 (2000) 948–954.
[7] D. Kolodyńska, The biodegradable complexing agents as an alternative to chelators in sorption of heavy metal ions, Desalin. Water Treat. 16 (2010) 146–155.
[8] A.S. Adeleye, A.A. Keller, R.J. Miller, H.S. Lenihan, Persistence of commercial nanoscaled zero-valent iron (nZVI) and by-products, J. Nanopart. Res. 15 (2013) 1–18.
[9] P.T.T. Thu, T.T. Thanh, H.N. Phi, S.J. Kim, V. Vo, Adsorption of lead from water by thiol-functionalized SBA-15 silicas, J. Mater. Sci. 45 (2010) 2952–2957.
[10] X. Sun, C. Hu, J. Qu, Adsorption and removal of arsenite on ordered mesoporous Fe-modified ZrO_2, Desalin. Water Treat. 8 (2009) 139–145.
[11] R.L. Frost, Y. Xi, H. He, Synthesis, characterization of palygorskite supported zero-valent iron and its application for methylene blue adsorption, J. Colloid Interface Sci. 341 (2010) 153–161.
[12] P. Rao, M.S. Mak, T. Liu, K.C. Lai, I. Lo, Effects of humic acid on arsenic(V) removal by zero-valent iron from groundwater with special references to corrosion products analyses, Chemosphere 75 (2009) 156–162.
[13] W. Zhang, D.W. Elliott, Applications of iron nanoparticles for groundwater remediation, Rem. J. 16 (2006) 7–21.
[14] B. Schrick, B.W. Hydutsky, J.L. Blough, T.E. Mallouk, Delivery vehicles for zerovalent metal nanoparticles in soil and groundwater, Chem. Mater. 16 (2004) 2187–2193.
[15] F. He, D. Zhao, J. Liu, C.B. Roberts, Stabilization of Fe−Pd nanoparticles with sodium carboxymethyl cellulose for enhanced transport and dechlorination of trichloroethylene in soil and groundwater, Ind. Eng. Chem. Res. 46 (2007) 29–34.
[16] S. Buendía, G. Cabañas, G. Álvarez-Lucio, H. Montiel-Sánchez, M. Navarro-Clemente, M. Corea, Preparation of magnetic polymer particles with nanoparticles of Fe (0), J. Colloid Interface Sci. 354 (2011) 139–143.
[17] K. Siskova, J. Tucek, L. Machala, E. Otyepkova, J. Filip, K. Safarova, J. Pechousek, R. Zboril, Air-stable nZVI formation mediated by glutamic acid: Solid-state storable material exhibiting 2D chain morphology and high reactivity in aqueous environment, J. Nanopart. Res. 14 (2012) 1–13.
[18] P. Calvo, C. Remunan-Lopez, J. Vila-Jato, M. Alonso, Novel hydrophilic chitosan-polyethylene oxide nanoparticles as protein carriers, J. Appl. Polym. Sci. 63 (1997) 125–132.
[19] B. Geng, Z. Jin, T. Li, X. Qi, Preparation of chitosan-stabilized Fe^0 nanoparticles for removal of hexavalent chromium in water, Sci. Total Environ. 407 (2009) 4994–5000.
[20] R. Singh, V. Misra, R.P. Singh, Synthesis, characterization and role of zero-valent iron nanoparticle in removal of hexavalent chromium from chromium-spiked soil, J. Nanopart. Res. 13 (2011) 4063–4073.
[21] A. Gupta, M. Yunus, N. Sankararamakrishnan, Zero-valent iron encapsulated chitosan nanospheres—A novel adsorbent for the removal of total inorganic Arsenic from aqueous systems, Chemosphere 86 (2012) 150–155.
[22] X. Liu, Q. Hu, Z. Fang, X. Zhang, B. Zhang, Magnetic chitosan nanocomposites: A useful recyclable tool for heavy metal ion removal, Langmuir 25 (2008) 3–8.

[23] Y. Wan, H. Wu, A. Yu, D. Wen, Biodegradable polylactide/chitosan blend membranes, Biomacromolecules 7 (2006) 1362–1372.
[24] Y.Y. Liang, L.M. Zhang, Bioconjugation of papain on superparamagnetic nanoparticles decorated with carboxymethylated chitosan, Biomacromolecules 8 (2007) 1480–1486.
[25] N. Horzum, M.M. Demir, M. Nairat, T. Shahwan, Chitosan fiber-supported zero-valent iron nanoparticles as a novel sorbent for sequestration of inorganic arsenic, RSC Adv. 3 (2013) 7828–7837.
[26] L.B. Hoch, E.J. Mack, B.W. Hydutsky, J.M. Hershman, J.M. Skluzacek, T.E. Mallouk, Carbothermal synthesis of carbon-supported nanoscale zero-valent iron particles for the remediation of hexavalent chromium, Environ. Sci. Technol. 42 (2008) 2600–2605.
[27] Y.H. Lin, H.H. Tseng, M.Y. Wey, M.D. Lin, Characteristics of two types of stabilized nano zero-valent iron and transport in porous media, Sci. Total Environ. 408 (2010) 2260–2267.
[28] I. Capek, Preparation of metal nanoparticles in water-in-oil (w/o) microemulsions, Adv. Colloid Interface Sci. 110 (2004) 49–74.
[29] N. Saleh, K. Sirk, Y. Liu, T. Phenrat, B. Dufour, K. Matyjaszewski, R.D. Tilton, G.V. Lowry, Surface modifications enhance nanoiron transport and NAPL targeting in saturated porous media, Environ. Eng. Sci. 24 (2007) 45–57.
[30] P. Wu, W. Wu, S. Li, N. Xing, N. Zhu, P. Li, J. Wu, C. Yang, Z. Dang, Removal of Cd^{2+} from aqueous solution by adsorption using Fe-montmorillonite, J. Hazard. Mater. 169 (2009) 824–830.
[31] G. Tan, D. Xiao, Adsorption of cadmium ion from aqueous solution by ground wheat stems, J. Hazard. Mater. 164 (2009) 1359–1363.
[32] Q. Qin, Q. Wang, D. Fu, J. Ma, An efficient approach for Pb(II) and Cd(II) removal using manganese dioxide formed *in situ*, Chem. Eng. J. 172 (2011) 68–74.
[33] S.R. Kanel, B. Manning, L. Charlet, H. Choi, Removal of arsenic(III) from groundwater by nanoscale zero-valent iron, Environ. Sci. Technol. 39 (2005) 1291–1298.
[34] S.M. Ponder, J.G. Darab, T.E. Mallouk, Remediation of Cr(VI) and Pb(II) aqueous solutions using supported, nanoscale zero-valent iron, Environ. Sci. Technol. 34 (2000) 2564–2569.
[35] K.G. Bhattacharyya, S.S. Gupta, Adsorptive accumulation of Cd(II), Co(II), Cu(II), Pb(II), and Ni(II) from water on montmorillonite: Influence of acid activation, J. Colloid Interface Sci. 310 (2007) 411–424.
[36] G. Mckay, H. Blair, J. Gardner, Adsorption of dyes on chitin. I. Equilibrium studies, J. Appl. Polym. Sci. 27 (1982) 3043–3057.
[37] Y. Liu, Z. Liu, J. Gao, J. Dai, J. Han, Y. Wang, J. Xie, Y. Yan, Selective adsorption behavior of Pb(II) by mesoporous silica SBA-15-supported Pb(II)-imprinted polymer based on surface molecularly imprinting technique, J. Hazard. Mater. 186 (2011) 197–205.
[38] Y.J. Tu, C.F. You, C.K. Chang, Kinetics and thermodynamics of adsorption for Cd on green manufactured nano-particles, J. Hazard. Mater. 235–236 (2012) 116–122.
[39] T. Tay, M. Candan, M. Erdem, Y. Çimen, H. Türk, Biosorption of cadmium ions from aqueous solution onto non-living Lichen *Ramalina fraxinea* biomass, Clean Soil Air Water 37 (2009) 249–255.
[40] K.S. Rao, S. Anand, P. Venkateswarlu, Adsorption of cadmium (II) ions from aqueous solution by Tectona grandis LF (teak leaves powder), BioResources 5 (2010) 438–454.
[41] X. Li, W. Zhang, Sequestration of metal cations with zerovalent iron nanoparticles—A study with high resolution X-ray photoelectron spectroscopy (HR-XPS), J. Phys. Chem. C 111 (2007) 6939–6946.
[42] H.L. Vasconcelos, T.P. Camargo, N.S. Gonçalves, A. Neves, M. Laranjeira, V.T. Fávere, Chitosan crosslinked with a metal complexing agent: Synthesis, characterization and copper(II) ions adsorption, React. Funct. Polym. 68 (2008) 572–579.